Sentinel 1 raw IQ stream processing beyond Synthetic Aperture RADAR applications

Jean-Michel Friedt JMFRIEDT@FEMTO-ST.FR
FEMTO-ST/Time & Frequency, Besançon, France

Abstract

A free, opensource Sentinel1 Level0 decoder is described providing access to the raw IQ data transmitted by the spaceborne RADAR satellites prior to range and azimuth compression. Most importantly, rank echoes when emitted pulses have not yet returned to the spaceborne RADARs allow for listening to ground based emissions – most significantly civilian (weather) and military RADARs, as well as for radiometric measurements.

1. Introduction

Sentinel1 (ESA, 2012) is a set of spaceborne RADARs operated by the European Space Agency (ESA). The C-band (centered on 5.405 GHz) radiofrequency {I,Q} datastreams are relayed by the European Data Relay Satellites (EDRS) before being received by ESA listening stations, processed and stored for being disseminated to users. Indeed, the current data policy of ESA is to freely share data to foster economic development beyond a closed source approach limiting dissemination to a few lucky selected.

While ESA will provide free of charge the Level1 (Piantanida, 07/06/2019) processed synthetic aperture RADAR (SAR) data, raw Level0 IQ streams are not supported. Nevertheless, ESA is providing access to these data, leaving to the user the task of decoding, decompressing and analyzing the raw data. We will discuss here how the packetized and compressed data have been analyzed, providing access beyond SAR analysis thanks to the rank echoes when the spaceborne radiofrequency receiver only listens to signals emitted from the Earth before any reflected echo is returned. In this mode, Sentinel1 acts as a radiometer or a listener of ground based emissions, most commonly from C-band civilian or G-band military RADARs.

Proceedings of the 3^{rd} *European GNU Radio Days*,

2. CCSDS packets

Sentinel satellites being Low Earth Orbiting (LEO) space vehicles flying at 700 km from the surface of the planet, their coverage is only a minute fraction of the surface of the Earth and continuous reception of their datastream would require deploying numerous receiving stations, most challenging over vast areas of ocneanic water expanses as was done in the early days of the Space Exploration (Hacker & Grimwood, 1977). Similar to the American TDRS, Europe has deployed EDRS relay satellites in geostationary orbit to relay LEO satellite signals and route them to the receivers located in Europe or in the United Kingdom (UK). Thus, multiple instruments from multiple space vehicles are transmitting through EDRS, requiring some sort of identification of the signal source as encoded in the Consultative Committee for Space Data Systems (CCSDS) packets (Flachs, 22/05/2015). The data format organization is immediately assessed by searching for the synchronization word 0x352EF853 in the raw datasets (Fig. 1) downloaded from ESA Copernicus Hub web site: finding this synchronization word validates the CCSDS packet structure whose primary and secondary headers are fixed length. The data payload being compressed, the challenge lies in implementing the adaptative decompression algorithm implemented as a Huffman tree decoding with 5 different trees being selected depending on the resolution of features to be conveyed, with the highest resolution over urban areas and weakest resolution over forest and wide vegetations expanses.

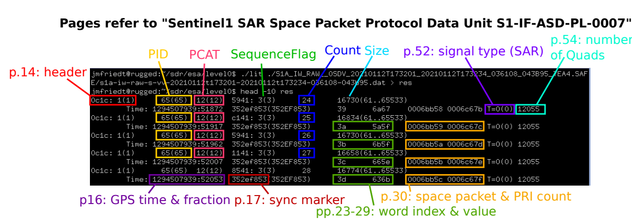

Figure 1. Analyzing the hexadecimal dump of a raw Sentinel1 binary file with respect to the CCSDS packet structure.

The interleaved I and Q datasets are readily decompressed and the proper datalength with respect to the expected number of data pairs NQ validates that decompression was completed properly. In this analysis, the hardware layer of data transfer (forward error correction such as Viterbi and Reed Solomon error correction) has already been taken care of by ESA receivers and we assume that the files are not corrupt.

3. Data quality assessment

3.1. Bit Rate Code (BRC) maps

Decompression results is a stream of I and Q data whose validity is to be assessed. One approach considered in the literature (Guccione et al., 2015) is to only analyze the compression factor and its relation to the features of ground reflectors. Indeed mapping the Bit Rate Coding (BRC) factor indicates some regional features with strong compression ratios and other features with weaker ratio and higher fidelity associated with urban areas (Fig. 2).

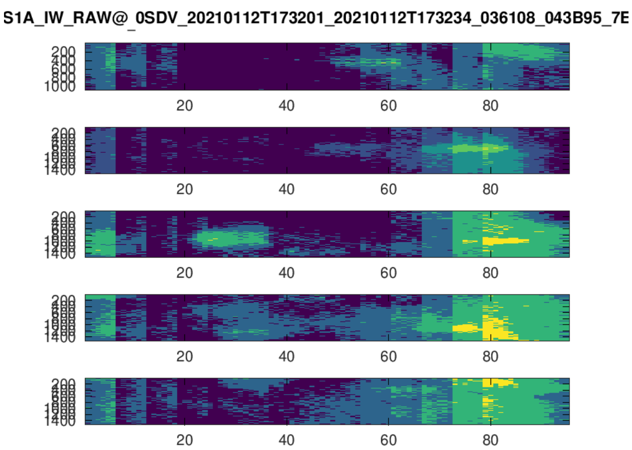

Figure 2. Bit Rate Code (BRC) map.

3.2. Range compression

BRC mapping demonstrates proper data sub-block analysis but does not demonstrate proper Huffman decoding implementation. Huffman decoding of the unbalanced trees used by ESA is implemented and finite state machines mostly counting the number of ones in the data word since zero will most often indicate a leaf of the tree has been reached, followed by a quantization step. Reaching an inexisting code sequence hints at an erroneous implementation of the Huffman decoding scheme or bit padding of the blocks. On the other hand, reaching the expected NQ number of quads of IQ data hints at a proper implementations.

Sentinel1 provides, in addition to the IQ stream, telemetry information including attitude (one parameter for each

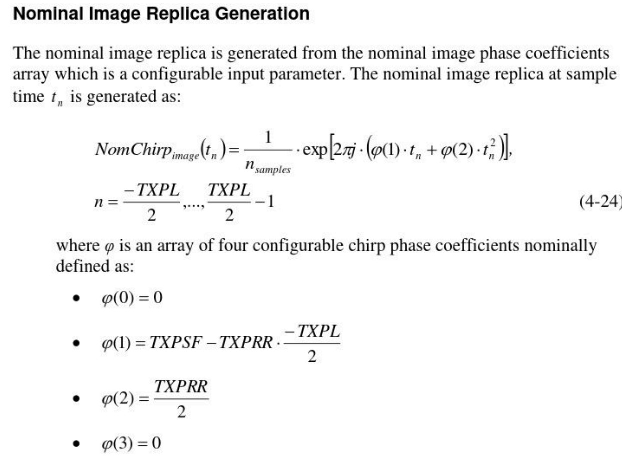

Nominal Image Replica Generation

The nominal image replica is generated from the nominal image phase coefficients array which is a configurable input parameter. The nominal image replica at sample time t_n is generated as:

$$NomChirp_{image}(t_n) = \frac{1}{n_{samples}} \cdot \exp\left[2\pi j \cdot \left(\varphi(1) \cdot t_n + \varphi(2) \cdot t_n^2\right)\right],$$
$$n = \frac{-TXPL}{2}, \ldots, \frac{TXPL}{2} - 1 \quad (4\text{-}24)$$

where φ is an array of four configurable chirp phase coefficients nominally defined as:

- $\varphi(0) = 0$
- $\varphi(1) = TXPSF - TXPRR \cdot \frac{-TXPL}{2}$
- $\varphi(2) = \frac{TXPRR}{2}$
- $\varphi(3) = 0$

Figure 3. Chirp phase evolution with illumination beam position related to telemetry paramters as provided by the documentation.

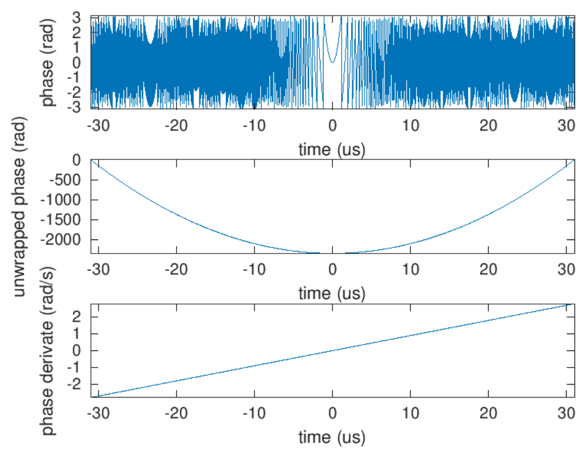

Figure 4. Chirp shape as deduced from the telemetry decoding, closely matching the impulse response of a point-like target in the range direction.

packet), transmitted pulse properties and transmission interval. Based on this telemetry information (Fig. 3), a local copy of the chirp is reconstructed and cross-correlated with the collected datasets in the range direction (Fig. 4).

Pulse compression in which the energy spread over time (Fig. 5) is accumulated in a single sample demonstrates proper telemetry decoding and proper IQ stream analysis. Comparing the fine match between the predicted unwrapped phase evolution as a function of space vehicle position with the phase evolution around a point-like target confirms the proper pulse shape decoding (Fig. 6).

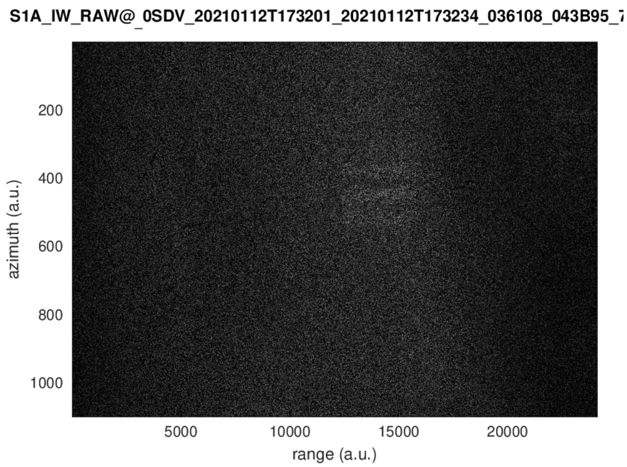

Figure 5. Raw IQ magnitude prior to range and azimuth compression, with energy spread around targets.

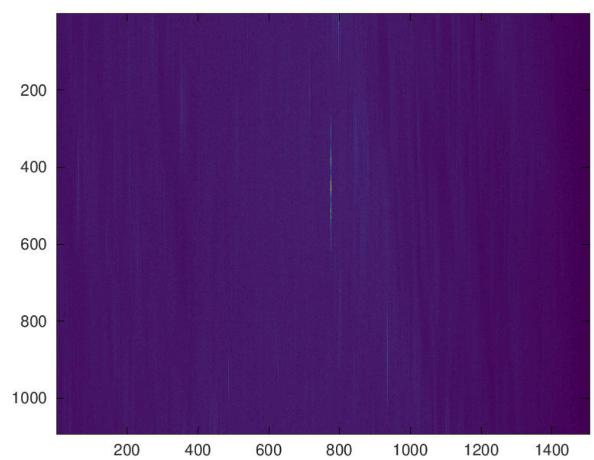

Figure 6. Range compression, with energy spread in the range direction accumulated in a single pixel in the case of the point-like target of a ship waiting in the harbour of Sao Paolo.

3.3. Azimuth compression

Azimuth compression is more challenging since in addition to relying on the pulse repetition rate acting as sampling frequency in the azimuth direction, spaceborne SAR theoretical background is needed (Sandwell et al., 2016). Based on the literature, the phase parabolic shape curvature is deduced from space vehicle speed and altitude, again matching finely the observed phase variation along the azimuth direction. Indeed we are taught in (Sandwell et al., 2016) (p.55, Eq. B13) that an effective speed is given by

$$v_e = \frac{v_s}{\sqrt{1 + \frac{Hleo}{REarth}}}$$

determined from the radius of the Earth $REarth$, the altitude of the satellite orbit $Hleo$ and its linear velocity v_s as computed from the ratio of its orbit circumference to the period, for exampled derived from the third Kepler law or from Two Line Element orbital parameters. This effective speed leads to $R_0\ddot{R} = v_e^2$ with R_0 the beam path determined as the satellite altitude divided by the cosine of the illumination angle (about 45° for Sentinel1) and finally the phase curvature is $\ddot{R} = v_e^2/R_0 = 52.7$ m/s^2 which is close to the value tabulated in (Sandwell et al., 2016) (p.59, Fig. B12). The phase change rate (derivate of the parabolic law) is hence $-4\pi/\lambda \times \ddot{R} \times dt$ with dt the time interval between two measurents as determined by the pulse repetition rate and λ the electromagnetic wavelength $300/5405 = 0.055$ m.

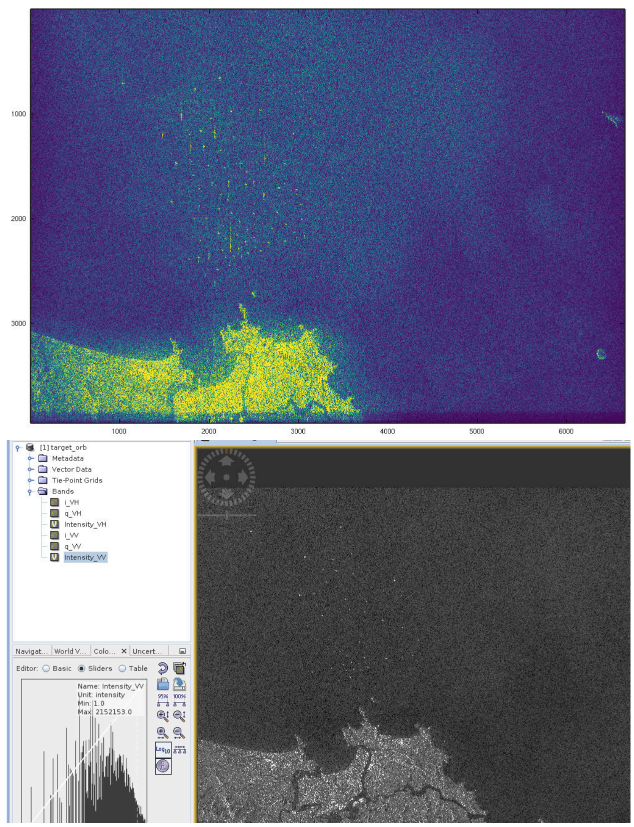

Figure 7. Comparison of the range-azimuth compression result applied to the raw Level0 decoded datasets, and for the same acquisition the Level1 dataset published by ESA and loaded with the Sentinel Application Platform (SNAP) software.

Correlating the range-compressed image with this phase parabolic shape along the azimuth direction leads to the result exhibited in Fig. 7 (top) which favorably compares with the Level1 datasets published by ESA and here processed with the Sentinel Application Platform (SNAP) software (bottom), demonstrating our proper understanding of the Level0 data analysis and processing.

4. Beyond SAR analysis

Having demonstrated proper decoding of raw Level0 Sentinel1 data, we might address their use beyond the classical SAR analysis. Our initial objective with this investigation was reproducing the results published in (Monti-Guarnieri et al., 2017) and (*& al.*, 2019). Indeed, Sentinel1 starts recording receiver signals as soon as chirped pulses are being transmitted. However, emitted pulses will require some time to return: the listening duration with no returned echoes are called *rank echoes*.

Although the analysis of rank echoes cannot aim at achieving the high spatial localization results expected from the French Ceres constellation (*Capacité de REnseignement Électromagnétique Spatial*) (des Armées), at least data are available for analysis and searching for signals. As demonstrations of this path of investigation, on the one hand radiometric measurements hint at the power returned from sea or ground covered areas below the flight path, and some periodic signals might be associated with ground based civilian RADARs since the signature hints at a match with C-band weather RADARs.

Downloading all raw datasets of a pass over Europe and processing the rank echo levels demonstrates how the background noise drops over sea surfaces and rises over ground (Fig. 8).

Amongst the many possibilities offered by accessing the raw IQ data, wind speed has been measured by finely analyzing the Doppler shift of the air layers met by the electromagnetic pulses on their trip to and from the surface of the Earth (Mouche et al., 2012; Ahsbahs, 2020), while ground (Harel, 2018) and sea (Sutton, 2020) military RADARs are readily detected and their characteristics deduced from the rank echo analysis.

5. Conclusion

Thanks to the availability of the raw Level0 datasets on the ESA Copernicus Hub and the associated documentation, a decoder of these files is provided. Confidence in its functional capability is validated with range and azimuth compression as well as radiometric analysis of the rank echoes. Source codes are available at `https://github.com/jmfriedt/sentinel1_level0`.

References

Ahsbahs, T. Wind farm wakes from SAR and doppler radar. *MDPI Remote Sensing*, 12:462, 2020.

& al., N. Franceschi. Rfi monitoring and classificationin c-band using sentinel-1 noise pulses. 2019. `http://www.ursi.org/proceedings/2019/rfi2019/23p4.pdf`.

des Armées, Ministère. Projet de loi de programmation militaire 2019/2025 – dossier de presse. `https://www.defense.gouv.fr/content/download/523147/8769249/file/DP%20LPM%202019-2025.pdf`.

ESA. Sentinel-1 – ESA's radar observatory mission for GMES operational services. *SP-1322/1*, pp. 20, March 2012. `https://sentinel.esa.int/documents/247904/349449/S1_SP-1322_1.pdf`.

Flachs, H. Sentinel-1 SAR instrument – SAR space packet protocol data unit. *ESA*, 22/05/2015. `https://sentinel.esa.int/documents/247904/2142675/Sentinel-1-SAR-Space-Packet-Protocol-Data-Unit.pdf/d47f3009-a37a-43f9-8b65-da858f6fb1ca?t=1547146144000`.

Guccione, Pietro, Belotti, Michele, Giudici, Davide, Guarnieri, Andrea Monti, and Navas-Traver, Ignacio. Sentinel-1A: analysis of FDBAQ performance on real data. *IEEE Transactions on Geoscience and Remote Sensing*, 53(12):6804–6812, 2015.

Hacker, B.C. and Grimwood, J.M. *On the shoulders of titans – a history of project Gemini*. NASA, 1977. `https://history.nasa.gov/SP-4203.pdf`.

Harel, D. X marks the spot: Identifying MIM-104 Patriot batteries from Sentinel-1 SAR multi-temporal imagery, 2018. `https://medium.com/@HarelDan/x-marks-the-spot-579cdb1f534b`.

Monti-Guarnieri, Andrea, Giudici, Davide, and Recchia, Andrea. Identification of C-band radio frequency interferences from Sentinel-1 data. *Remote Sensing*, 9(11): 1183, 2017.

Mouche, Alexis A, Collard, Fabrice, Chapron, Bertrand, Dagestad, Knut-Frode, Guitton, Gilles, Johannessen, Johnny A, Kerbaol, Vincent, and Hansen, Morten Wergeland. On the use of doppler shift for sea surface wind retrieval from SAR. *IEEE Transactions on Geoscience and Remote Sensing*, 50(7):2901–2909, 2012.

Piantanida, R. Level 1 detailed algorithm definition. *ESA*, 07/06/2019. `https://sentinel.esa.int/documents/247904/1877131/Sentinel-1-Level-1-Detailed-Algorithm-Definition`.

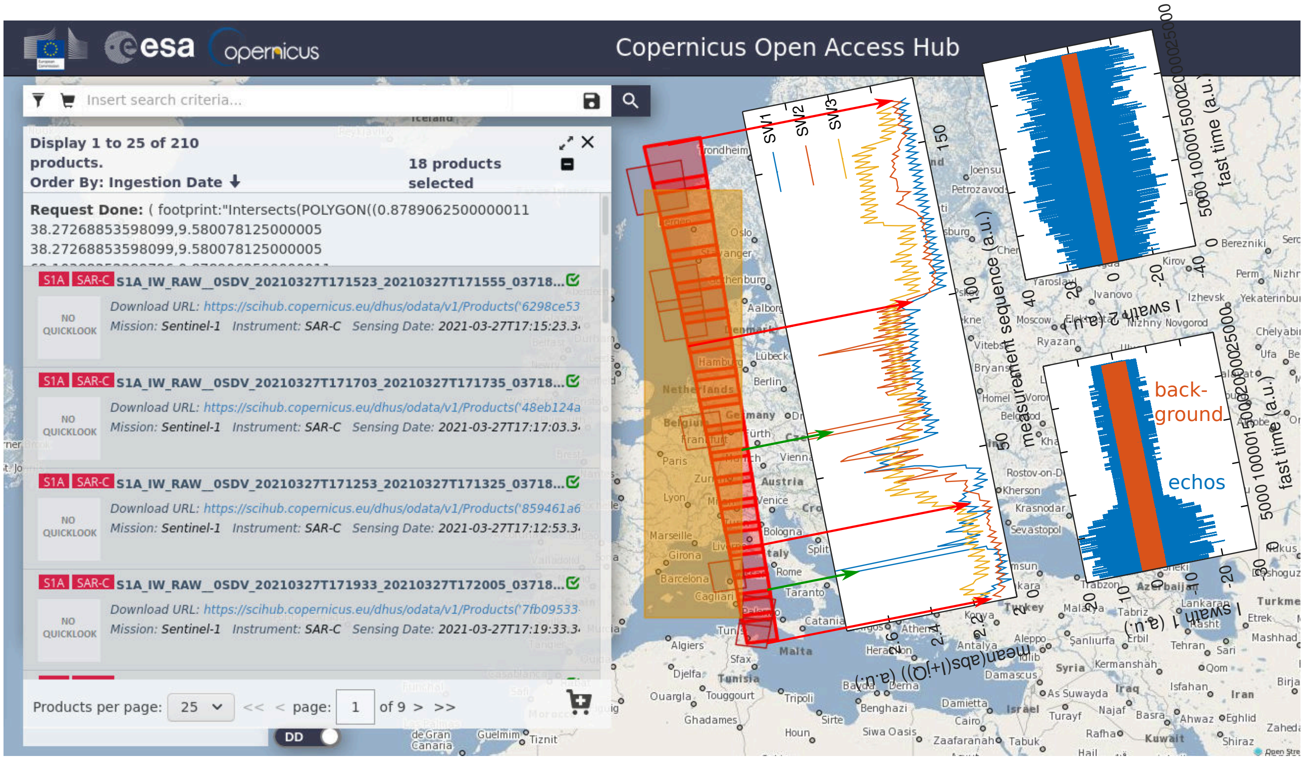

Figure 8. Mapping the power radiated from the ground towards Sentinel1 as measured in the rank echoes (red curves). For comparison, the echo level after waiting enoug time for the two-way trip echo duration is shown in blue on the right-most curve. The power level matches the path followed by Sentinel1, with received power dropping over the Mediteranean or Scandinavian seas.

Sandwell, David, Mellors, Rob, Tong, Xiaopeng, Wei, Matt, and Wessel, Paul. Gmtsar: An InSAR processing system based on generic mapping tools (2nd ed.). pp. 51–59, 2016. https://topex.ucsd.edu/gmtsar/tar/GMTSAR_2ND_TEX.pdf.

Sutton, H.I. Hidden threat to navies: How freely available satellite imagery can track radars, 2020. https://www.navalnews.com/naval-news/2020/12/hidden-threat-to-navies-how-freely-available-satellite-imagery-can-track-radars.